Supporting Information

Marjoram et al. 10.1073/pnas.1424089112

SI Materials and Methods

Barrier Assay. To assess barrier defects, 120 hpf WT and mutant *aa51.3*^{pd1092} larvae were gavaged with a 1% solution of FITC-dextran (4,000 MW; Sigma). Barrier defects were experimentally induced in 120 hpf WT fish via cogavage of 25 mM EDTA alongside 1% FITC-dextran. Mutant *aa51.3*^{pd1092} larvae carrying the *TgBAC(tnfa:GFP)* were gavaged at 103 hpf (morpholino experiments) or 120 hpf (germ-free experiments) with a 1% solution of Texas red dextran (3,000 MW; Invitrogen). Larvae were mounted in 3% (wt/vol) methylcellulose and imaged 30 min after gavage by using an Imager M1 (Zeiss) epifluorescent microscope under the same magnification and gain settings for each experiment. ImageJ software (NIH) was used to measure the integrated fluorescence density in a region of interest (ROI) just posterior and dorsal to the intestinal bulb in the somitic region (white rectangle in Fig. 1 *H–J*). A background ROI was measured outside of the fish and subtracted from the somitic ROI. All values were normalized to the average values from each WT gavage group.

Antibodies and Imaging. The primary antibodies used were as follows: pan-cadherin (1/1200; Sigma), ZO-1 (1/500; Invitrogen), GFP (1/750; Aves), phalloidin-488, -568 and -647 (1/300; Invitrogen), and 4e8 (1/500; AbCam), 2f11 (1/500; AbCam). Secondary antibodies (Molecular Probes) were used at 1/300, and DAPI (Invitrogen) was used at 1/1000. WT and *uhrf1*^{pd1092} mutant larvae at 96, 103, and 120 hpf were first vibratome sectioned and stained with GFP, phalloidin, and DAPI.

All samples were imaged on a Leica SP5 confocal microscope with a 40×/1.25–0.75 HCX PL APO oil objective. Quantification of *TgBAC(tnfa:GFP)* fluorescence in anterior gut sections was performed by using ImageJ. Using the phalloidin signal to visualize the gut outline, the polygon tool was used to encircle the entire gut in cross-section, and then the integrated fluorescence density was measured in the GFP channel (Gut + Luminal fluorescence). Luminal GFP fluorescence was measured by using the polygon tool to trace the apical surface in the phalloidin channel and measure the integrated fluorescence density in the GFP channel. The luminal fluorescence was then subtracted from the Gut + Luminal fluorescence to acquire the epithelial integrated fluorescence density.

Embryo Dissociation and FACS. To isolate IECs, *TgBAC(cldn15la-GFP)pd1034* (qPCR) and *Tg(−4.5ifabp:DsRed)pd1000* (bisulfite sequencing) were used, as transgene expression is restricted to the intestine in WT and mutant larvae. Briefly, 120 hpf WT or *uhrf1*^{pd1092} mutant larvae were dissociated in 0.25% Trypsin (Gibco) and 300 μg/mL collagenase (Sigma) for 1.5 h at 28 °C, pipetting in 15-min intervals to facilitate dissociation into a single-cell suspension. Cell suspensions from *TgBAC(cldn15la-GFP)pd1034* fish were stained with propidium iodide (Invitrogen) and *Tg(−4.5ifabp:DsRed)pd1000* suspensions were stained with 7-aminoactinomycin D (7AAD; Sigma) and sorted on a BD FACSVantage sorter into Buffer RLT (Qiagen) for RNA isolation and qPCR analysis or genomic DNA lysis buffer (1 M Tris, pH 8.5, 0.5 M EDTA, 1% SDS, 1 M NaCl) for bisulfite sequencing. Genomic DNA samples were treated with proteinase K overnight at 55 °C, phenol-chloroform extracted, and resuspended in 20 μL of dH_2O for bisulfite sequencing analysis.

Mouse IECs were isolated as published by Bjerknes et al. (1), with modifications. Briefly, postweaning mouse intestine was isolated and flushed with cold HBSS. The intestinal tube was opened longitudinally and incubated in precooled HBSS + 30 mM EDTA for 15 min at 37 °C. After incubation, intestinal segments were manually shaken in HBSS + 30 mM EDTA to release small epithelial sheets. The sheets were washed twice in cold HBSS before adding Buffer RLT for RNA isolation.

qPCR Primers. Zebrafish qPCR primers used include the following: *elfa* 5′F, 5′-CTTCTCAGGCTGACTGTGC-3′; *elfa* 3′R, 5′-CCGCTAGGATTACCCTCC-3′; *tnfa* 5′F, 5′-CAGGGCAATCAACAAGATGG-3′, *tnfa* 3′R, 5′-TGGTCCTGGTCATCTCTCCA-3′; *mmp9* 5′F, 5′-GCTGCTCATGAGTTTGGACA-3′, *mmp9* 3′R, 5′-AGGGCCAGTTCTAGGTCCAT-3′; *il1b* 5′F, 5′-GGCTGTGTGTTTGGGAATCT-3′, *il1b* 3′R, 5′-TGATAAACCAACCGGGACA-3′.

qPCR for mouse samples was performed as described above and normalized to beta 2-microglobulin. Mouse primers used include the following: B2M 5′F, 5′-CTGTATGCTATCCAGAAAACCC-3′, B2M 3′R, 5′-TCACATGTCTCGATCCCAGTAG-3′; TNF 5′F, 5′-CACGCTCTTCTGTCTACTGA-3′, TNF3′R, 5′-ATCTGAGTGTGAGGGTCTGG-3′.

1. Bjerknes M, Cheng H (1981) Methods for the isolation of intact epithelium from the mouse intestine. *Anat Rec* 199(4):565–574.

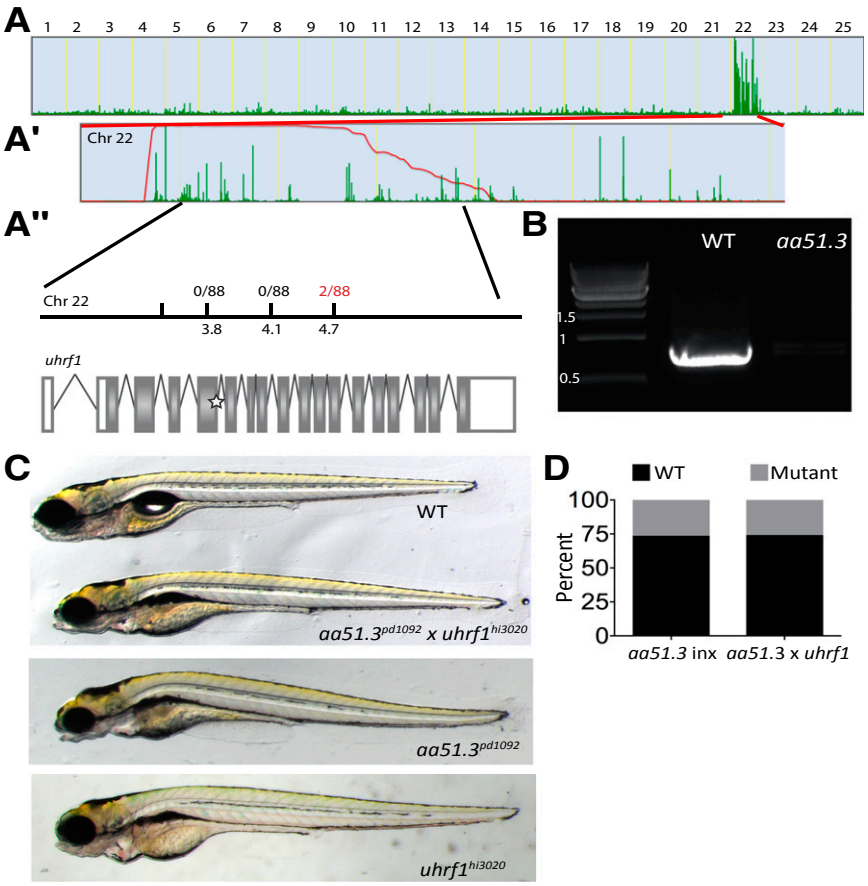

Fig. S1. Isolation of the *aa51.3*^{pd1092} locus. A splice-site mutation in *uhrf1* is causative of the *aa51.3*^{pd1092} phenotype. (*A*, *A*′, and *A*″) Whole exome sequencing of WT and *aa51.3*^{pd1092} larvae showing linkage to chromosome 22 in SNPTrack (*A*), the homozygosity interval (*A*′), and positional mapping of the region (*A*″), which identified a splice-site mutation in the splice donor site at the end of exon five (star) in *uhrf1*. (*B*) *uhrf1* exons 3 through 8 can be amplified in WT but not mutant larvae. (*C* and *D*) Noncomplementation of *aa51.3*^{pd1092} (*C*, *Middle*) with *uhrf1*^{hi3020} (*C*, *Bottom*). Brightfield image of noncomplementation (*C*) and quantification of failure to complement (*D*). (*D*: *aa51.3*^{pd1092} incross: $n = 90$ WT, $n = 33$ mutant; *aa51.3*^{pd1092}; *uhrf1*^{hi3020} complementation: $n = 250$ WT; $n = 89$ mutant).

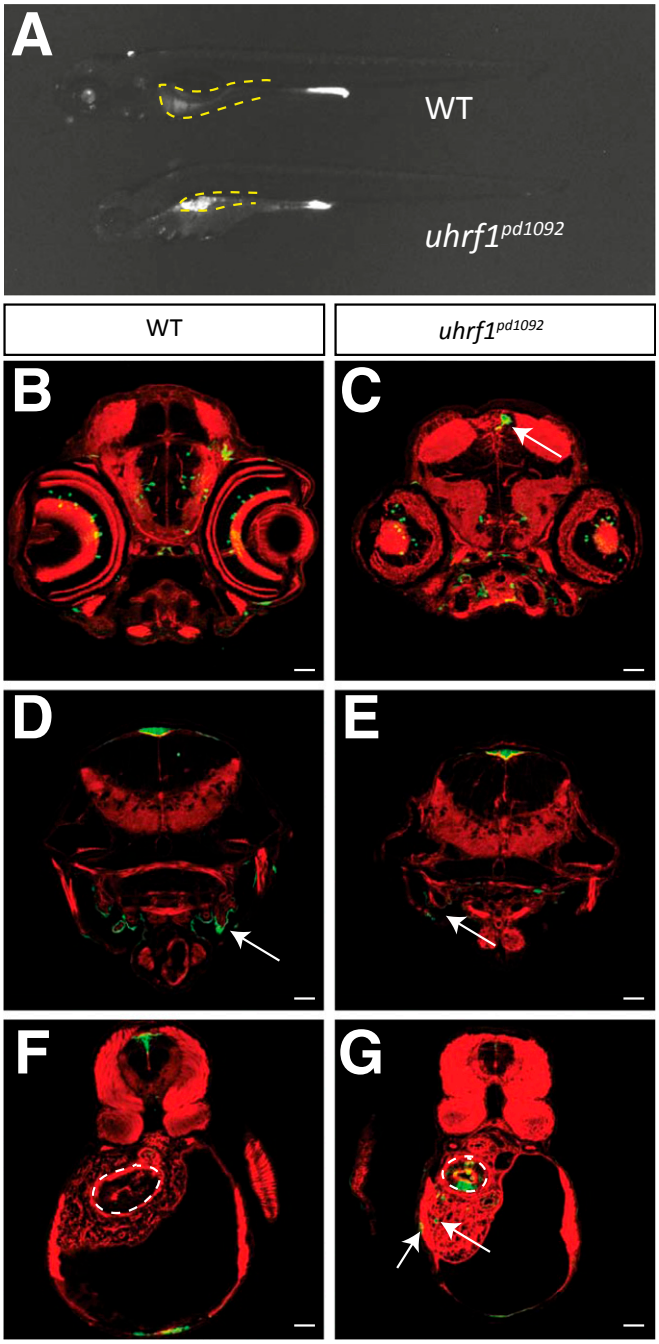

Fig. S2. *TgBAC(tnfa:GFP)* expression in WT and *uhrf1*^{pd1092} larvae. (*A*) Whole-mount image of WT and *uhrf1*^{pd1092} mutants showing the specificity of *TgBAC(tnfa:GFP)* up-regulation in the intestine (yellow dotted lines). (*B*–*G*) Confocal images of cross-sections stained with phalloidin (red). (*B* and *C*) Both WT and mutant larvae have GFP-positive cells in the brain and eye. The white arrow (*C*) points to an area of increased GFP expression in the mutant. (*D* and *E*) WT and mutant larvae express *TgBAC(tnfa:GFP)* in the gills (arrows). (*F* and *G*) Scattered GFP-positive cells are detected in the liver of mutants (*G*) but not in WT siblings. White dotted lines encircle the anterior gut; mutants display elevated *TgBAC(tnfa:GFP)* in the epithelium. (Scale bars: 50 μm.)

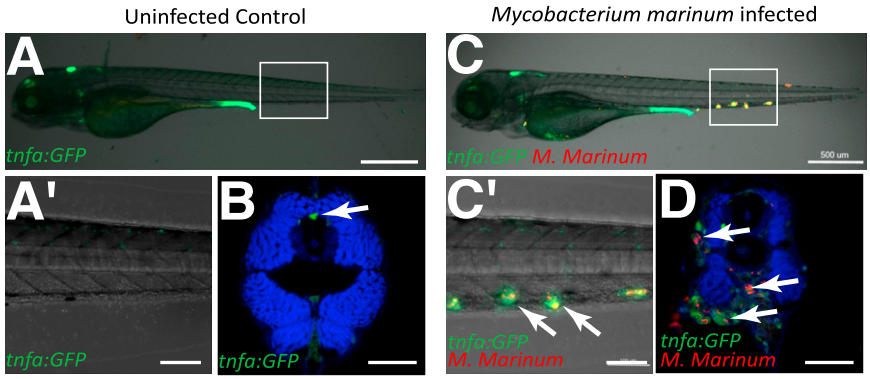

Fig. S3. *M. marinum* infection induces expression of *TgBAC(tnfa:GFP)* in WT larvae. (*A* and *A*′) Uninfected control *TgBAC(tnfa:GFP)* 120 hpf larvae at low magnification (*A*) and higher magnification of boxed area (*A*′). (*B*) Confocal image of a cross-section of an uninfected 120 hpf WT larva. Phalloidin, blue. Arrow points to basal *TgBAC(tnfa:GFP)* expression. (*C* and *C*′) *M. marinum*-infected (red) 120 hpf *TgBAC(tnfa:GFP)* larva at low magnification (*C*) and higher magnification of boxed area (*C*′). Arrows point to colocalization of *TgBAC(tnfa:GFP)* positive cells with *M. marinum*. (*D*) Cross-section through *M. marinum*-infected (red) 120 hpf *TgBAC(tnfa:GFP)* larva. Phalloidin, blue. Arrows point to *TgBAC(tnfa:GFP)*-positive granulomas surrounding *M. marinum* bacteria. (Scale bars: *A* and *C*, 500 μm; *A*′ and *C*′, 100 μm; *B* and *D*, 50 μm.)

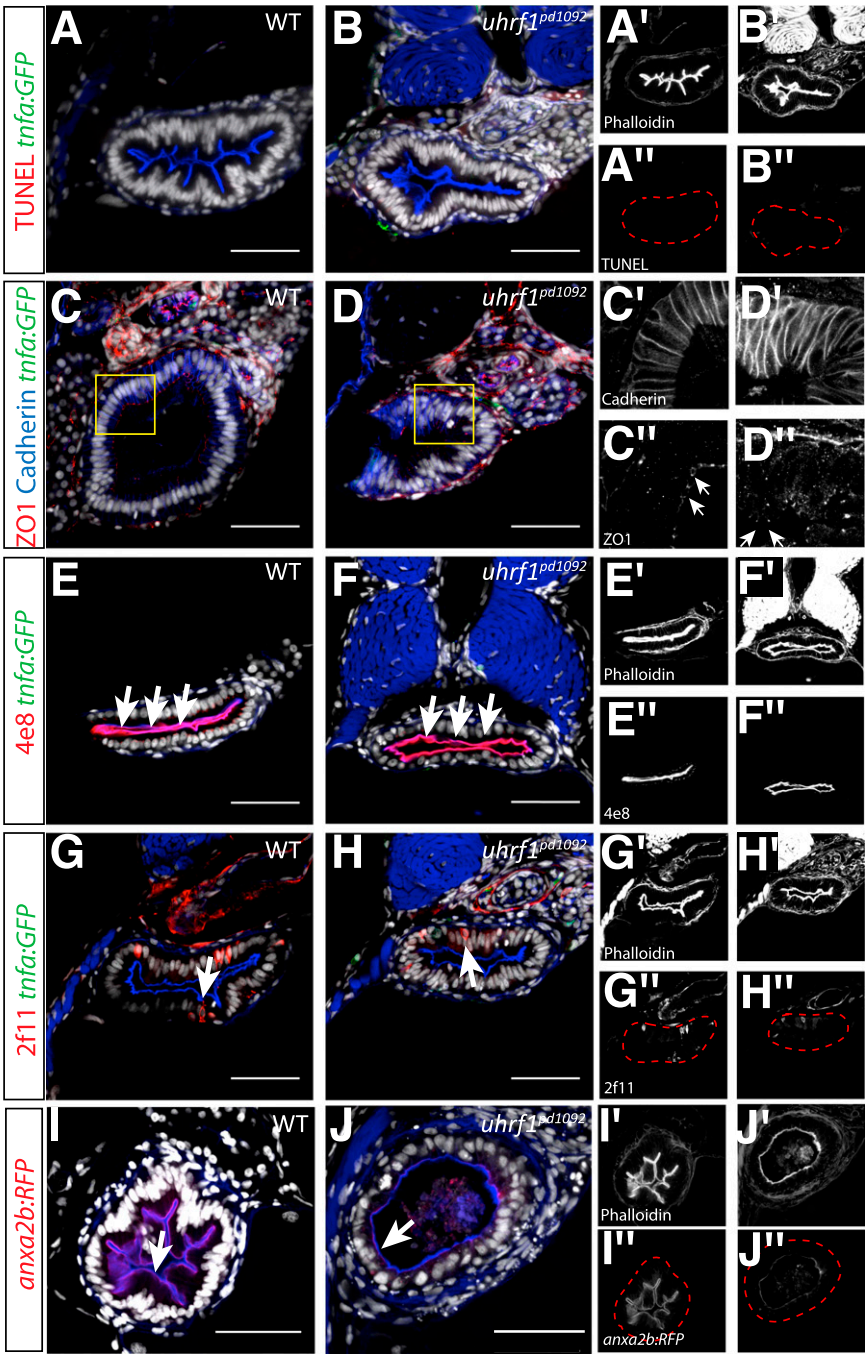

Fig. S4. *uhrf1*^{pd1092} intestines are morphologically indistinguishable from WT before *tnfa* elevation at 96 hpf. Shown are confocal images of cross-sections. (*A* and *B*) WT and mutant larvae stained for TUNEL. (*A′*, *A″*, *B′*, and *B″*) Typical epithelial morphology in WT (*A′*) and mutant (*B′*) larvae. No TUNEL-positive cells in WT (*A″*) or mutant (*B″*) larvae. WT (*C*) and mutant (*D*) larvae stained for pan-cadherin and ZO-1. (*C′*, *C″*, *D′*, and *D″*) Basolateral localization of pan-cadherin in WT (*C′*) and mutant (*D′*) larvae. Apical localization (arrows) of ZO-1 in WT (*C″*) or mutant (*D″*) larvae. WT (*E*) and mutant (*F*) larvae stained for mature apical membrane with 4e8 (arrows). (*E′*, *E″*, *F′*, and *F″*) Phalloidin staining in WT (*E′*) and mutant (*F′*) larvae. Apical membrane marked by 4e8 staining in WT (*E″*) or mutant (*F″*) larvae. Enteroendocrine cells in WT (*G*) and mutant (*H*) larvae marked by 2f11 (arrows). (*G′*, *G″*, *H′*, and *H″*) Phalloidin staining in WT (*G′*) and mutant (*H′*) larvae. 2f11 positive enteroendocrine cells in WT (*G″*) or mutant (*H″*) larvae. *TgBAC(anxa2b-RFP)* is a late marker of gut differentiation and is localized apically (arrows) in WT (*I*) and mutant (*J*) larvae at 120 hpf. Although the mutant phenotype is present, *TgBAC(anxa2b-RFP)* is expressed. (*I′*,*I″*, *J′*, and *J″*) Phalloidin staining in WT (*I′*) and mutant (*J′*) larvae. Apical *TgBAC(anxa2b-RFP)* in 120 hpf WT (*I″*) or mutant (*J″*) larvae. (Scale bars: 50 μm.)

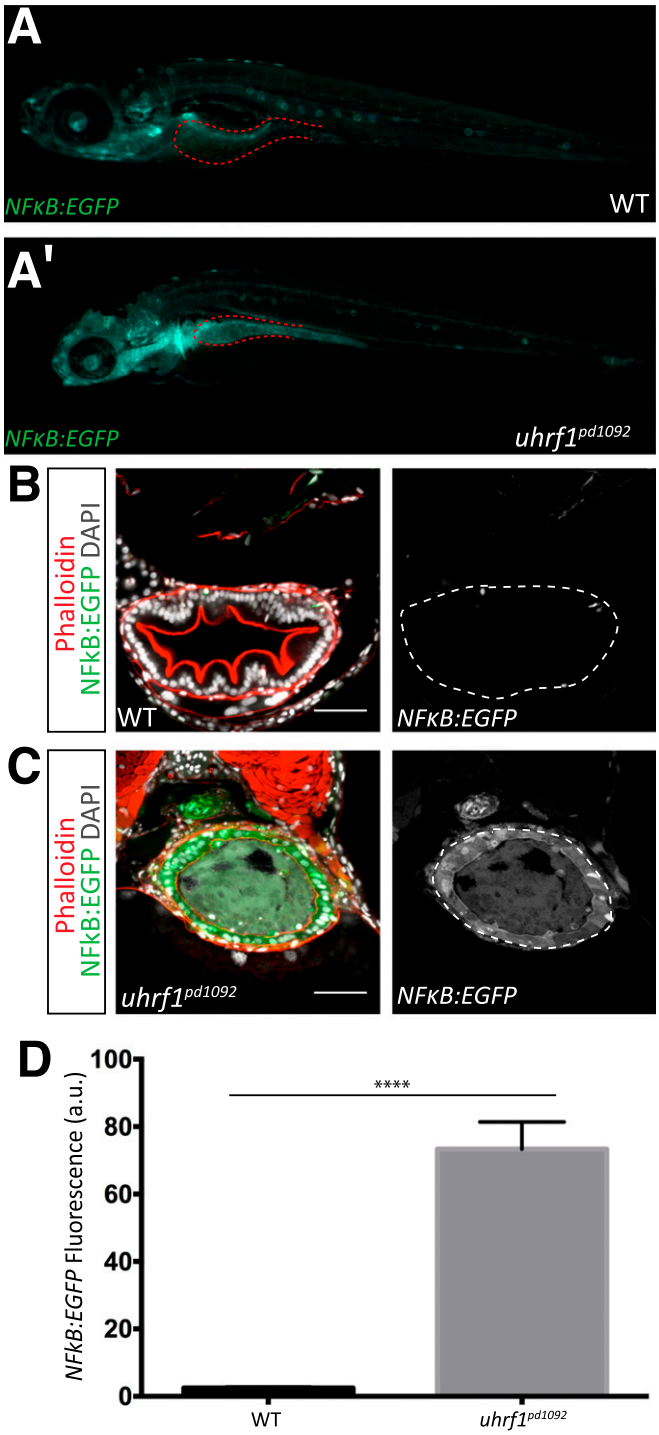

Fig. S5. Elevated *NFκB:EGFP* expression in the intestine of *uhrf1*^{pd1092} mutants. Intestinal expression of *Tg(NFκB:EGFP)* in WT (*A*) and *uhrf1*^{pd1092} (*A′*) mutants at 120 hpf. The intestine is highlighted by a red dotted line; expression is elevated in mutants. (*B* and *C*) Confocal images of cross-sections of WT (*B*) and mutant (*C*) larvae. Mutants have elevated *NFκB:EGFP* in the intestinal epithelium (white dotted line). (*D*) Quantification of *Tg(NFκB:EGFP)* intestinal fluorescence (measured in arbitrary units, a.u.) in WT and mutant larvae. ****$P < 0.0001$.

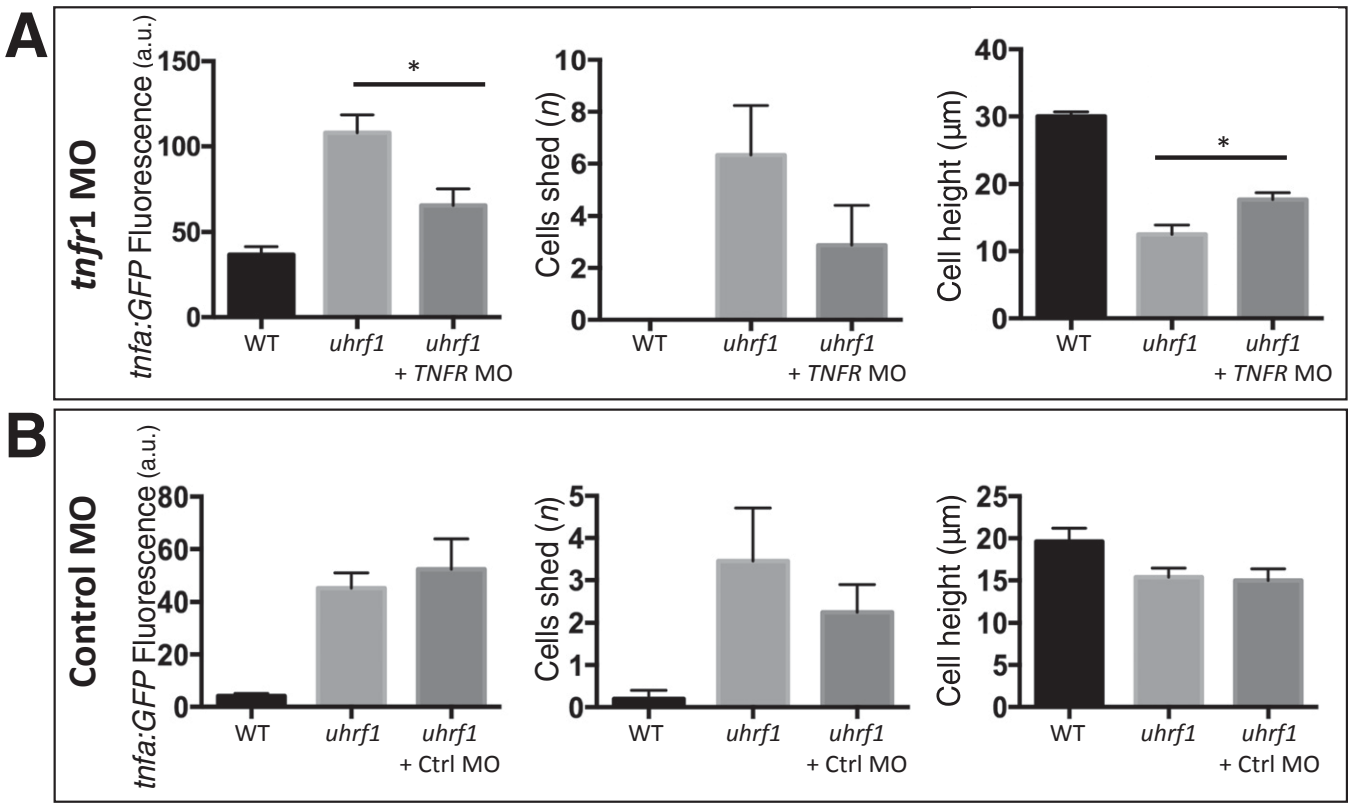

Fig. S6. Morpholino validation and controls. (*A*) Quantification of *tnfa:GFP* fluorescence (measured in arbitrary units, a.u.), cell shedding and cell height in *uhrf1*^{pd1092} mutants after injection of a morpholino against *tnfr1*. *tnfa:GFP* was decreased, whereas cell height was increased in morpholino-injected mutants. (*B*) No significant differences were observed in *tnfa:GFP* fluorescence (measured in arbitrary units, a.u.), cell shedding or cell height in mutants injected with a standard control morpholino. *$P < 0.05$.

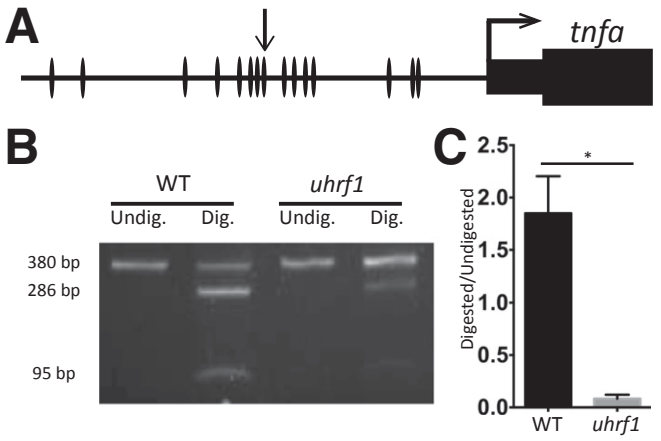

Fig. S7. COBRA analysis confirms hypomethylation of the *tnfa* promoter in *uhrf1*^{pd1092} mutants. (*A*) Schematic of zebrafish *tnfa* promoter, with CpG positions indicated. COBRA digestion site is marked with an arrow. (*B*) COBRA analysis of TaqαI cut-site (−712 bp) in WT and mutant samples. Digestion indicates methylation at this site. (*C*) Quantification of COBRA results represented by digested/undigested band intensity. Bars represent mean ± SEM; **$P < 0.0001$.

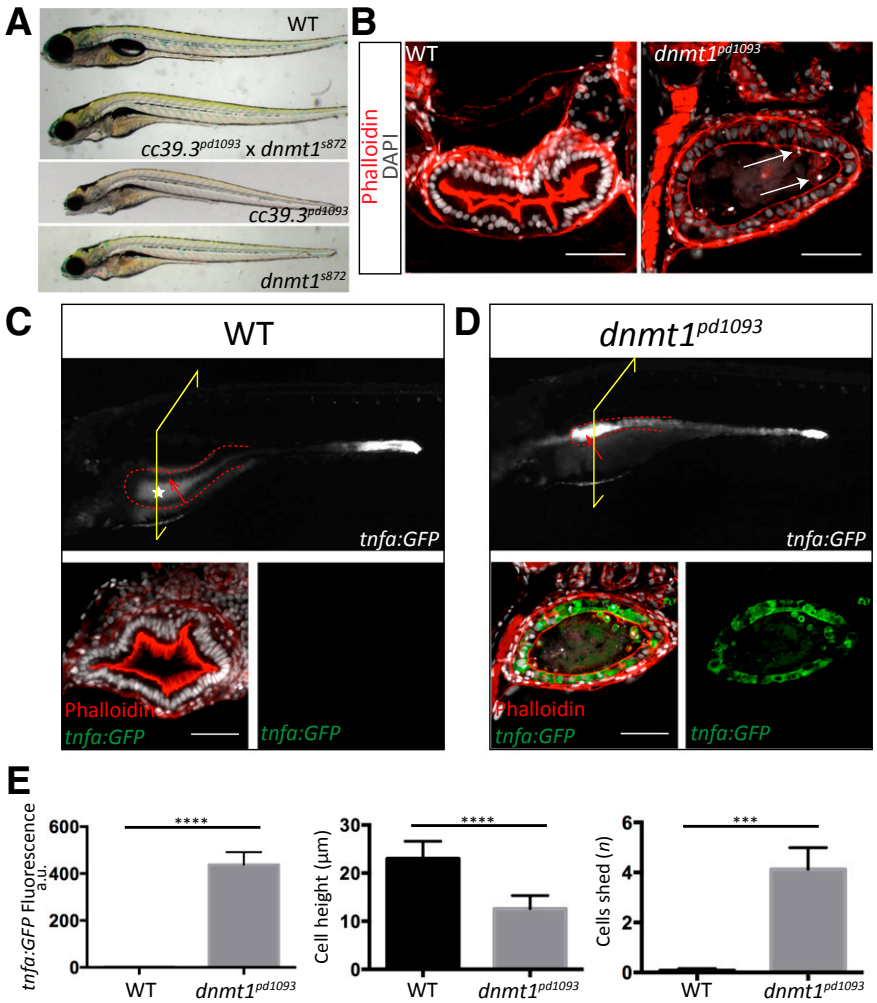

Fig. S8. A newly identified allele of *dnmt1* is similar to *uhrf1* and displays elevated *TgBAC(tnfa:GFP)* expression. (*A*) *cc39.3*^{pd1093} (*Middle*), a mutant recovered from our forward genetic screen, had a similar phenotype to *uhrf1*^{pd1092} and failed to complement (*Top*) with *dnmt1*^{s872} (*Bottom*). (*B*) Confocal images of cross-sections through WT and *dnmt1*^{pd1093} mutants revealed excessive cell shedding (arrows), luminal debris, and a flattened epithelium in mutants. (*C* and *D*) Elevated *TgBAC(tnfa:GFP)* expression was observed in the intestinal epithelium (encircled by a red dotted line) of *dnmt1*^{pd1093} mutants (*Upper* and *Lower Right*) but not WT larvae at 120 hpf. Red arrows point to the intestinal epithelium. The yellow frame indicates the plane of section for *C* and *D*, *Lower*. Cross-sections (*Lower*) through WT (*C*) and *dnmt1*^{pd1093} mutants (*D*) revealed up-regulation of *TgBAC(tnfa:GFP)* in the intestinal epithelium of mutants. (*E*) *dnmt1*^{pd1093} mutants have increased *TgBAC(tnfa:GFP)* epithelial fluorescence (measured in arbitrary units, a.u.), decreased cell height, and increased cell shedding, similar to *uhrf1*^{pd1092} mutants. ***$P < 0.001$, ****$P < 0.0001$.

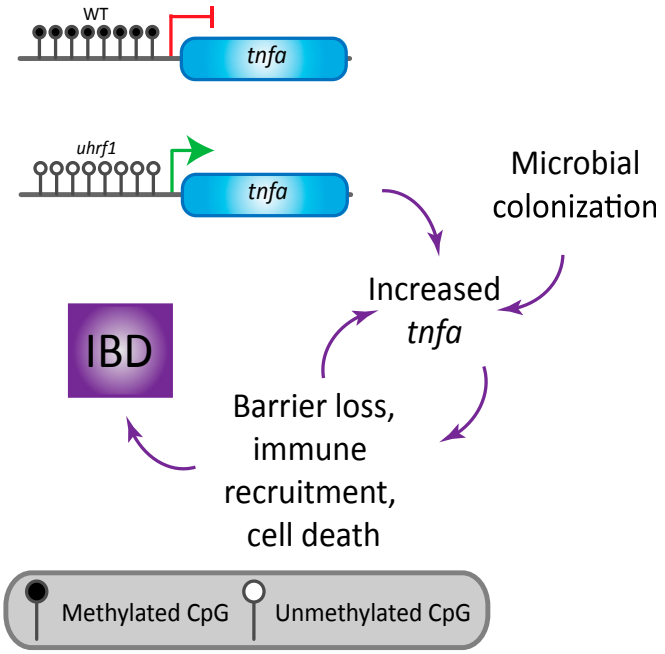

Fig. S9. Loss of *tnfa* promoter methylation leads to inflammation in the intestinal epithelium. Hypomethylation of the *tnfa* promoter due to loss of *uhrf1* function leads to elevated intestinal epithelial *tnfa* expression. Microbial colonization increases the *tnfa* levels, ultimately leading to barrier defects, immune recruitment, and cell death in the intestinal epithelium, and an IBD-like phenotype.

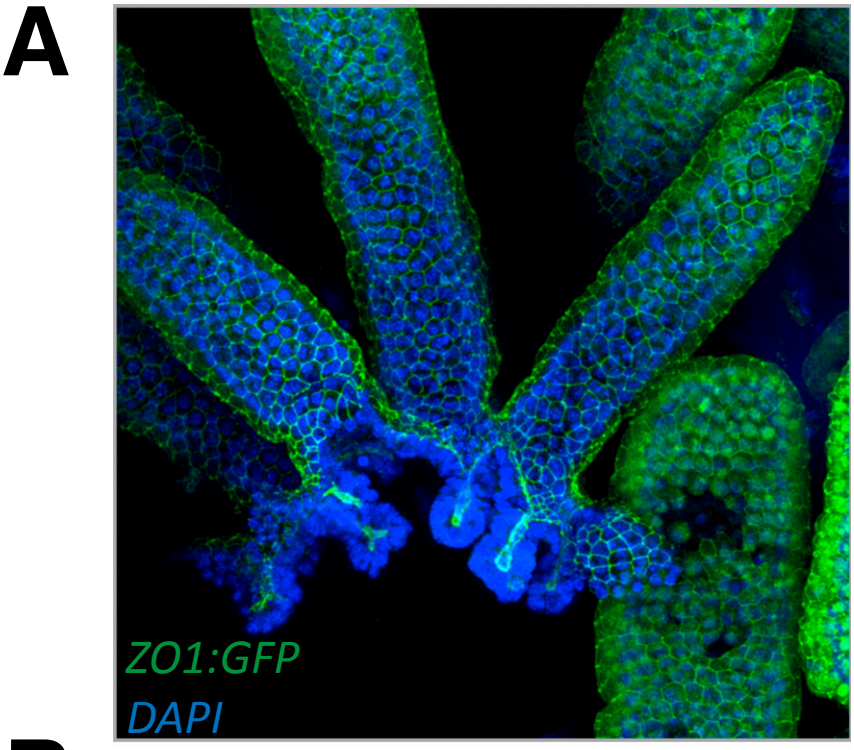

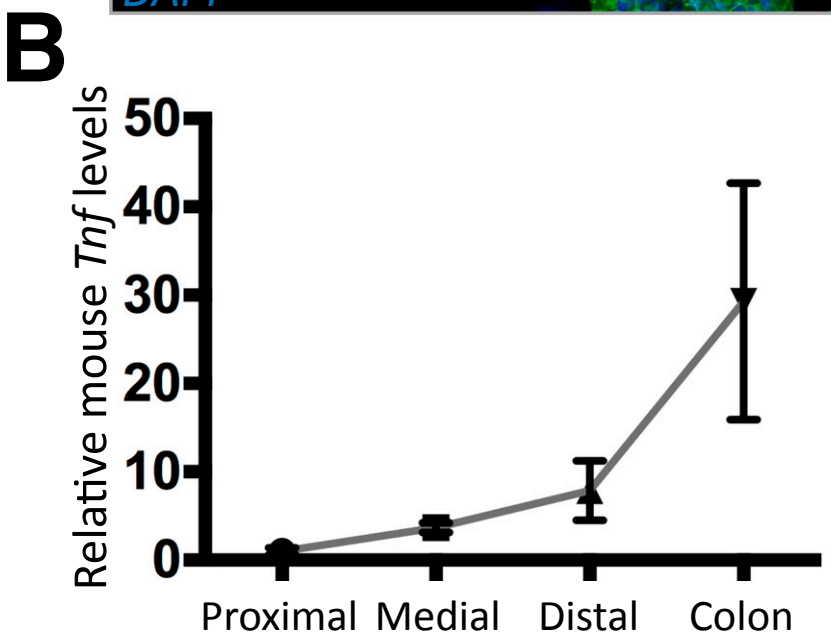

Fig. S10. *TNF* transcripts are more abundant in the colonic epithelium of mice compared with the small intestinal epithelium. (*A*) Image of an isolated mouse small intestinal epithelial sheet demonstrates enrichment of epithelial components and the absence of stromal and muscular elements. *ZO1:GFP* (green) labels IECs, whereas DAPI (blue) labels nuclei. (*B*) TNF expression was assayed in the proximal, medial, and distal intestine and colon IECs. Although there is a wide variation in TNF levels in the colon, *TNF* mRNA expression is higher in the colonic IECs compared with those of the small intestine.